Dielectron production: QGP versus photon-photon mechanism

Wolfgang Schäfer [1]

[1] Institute of Nuclear Physics, PAN, Kraków

ICHEP 2020
40th International Conference on High Energy Physics
Prague, Czech Republic (Virtual Conference) 28. July - 6. August 2020

Outline

Peripheral/ultraperipheral collisions

Weizsäcker-Williams fluxes of equivalent photons

electromagnetic dissociation of heavy nuclei

From ultraperipheral to semicentral collisions

dileptons from $\gamma\gamma$ production vs thermal dileptons from plasma phase

density matrix generalization of the Weizsäcker-Williams approach

M. Kłusek-Gawenda, R. Rapp, W. S. and A. Szczurek, Phys. Lett. B **790** (2019) 339 [arXiv:1809.07049 [nucl-th]].

Fermi-Weizsäcker-Williams equivalent photons

Heavy nuclei Au, Pb **have** $Z \sim 80$

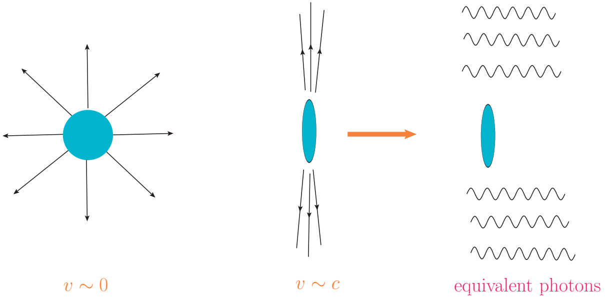

- ion at rest: source of a Coulomb field, the highly boosted ion: sharp burst of field strength, with $|\boldsymbol{E}|^2 \sim |\boldsymbol{B}|^2$ and $\boldsymbol{E} \cdot \boldsymbol{B} \sim 0$. (See e.g. J.D Jackson textbook).
- acts like a flux of "equivalent photons" (photons are collinear partons).

$$\boldsymbol{E}(\omega, \boldsymbol{b}) = -i \, \frac{Z\sqrt{4\pi\alpha_{em}}}{2\pi} \, \frac{\boldsymbol{b}}{b^2} \, \frac{\omega b}{\gamma} K_1\Big(\frac{\omega b}{\gamma}\Big) \; ; N(\omega, \boldsymbol{b}) = \frac{1}{\omega} \frac{1}{\pi} \Big| \boldsymbol{E}(\omega, \boldsymbol{b}) \Big|^2$$

$$\sigma(AB) = \int d\omega d^2\boldsymbol{b} \, N(\omega, \boldsymbol{b}) \, \sigma(\gamma B; \omega)$$

Finite size of particle → charge form factor

$$\boldsymbol{E}(\omega, \boldsymbol{b}) = Z\sqrt{4\pi\alpha_{em}} \int \frac{d^2\boldsymbol{q}}{(2\pi)^2} \exp[-i\boldsymbol{b}\boldsymbol{q}]\ \frac{\boldsymbol{q}}{\boldsymbol{q}^2 + \omega^2/\gamma^2}\ F_{em}(\boldsymbol{q}^2 + \omega^2/\gamma^2)$$

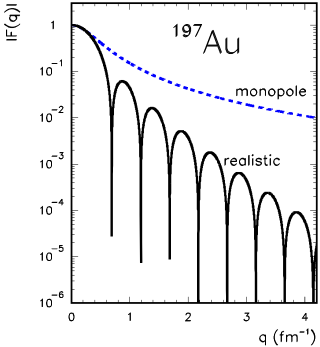

The modulus of the charge form factor $F_{em}(q)$ of the ^{197}Au nucleus for realistic charge distribution (solid). For comparison we show the monopole form factor often used in practical applications (dashed).

From M. Kłusek, W. S. and A. Szczurek, Phys. Lett. B **674** (2009), 92-97

Ultraperipheral collisions

some examples of ultraperipheral processes:

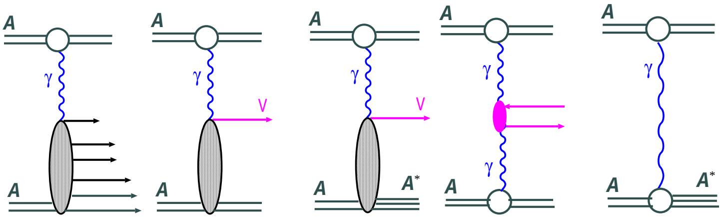

- photoabsorption on a nucleus
- diffractive photoproduction with and without breakup/excitation of a nucleus
- $\gamma\gamma$-fusion.
- electromagnetic excitation/dissociation of nuclei. Excitation of Giant Dipole Resonances.
- the intact nuclei in the final state are not measured. Each of the photon exchanges is associated with a large rapidity gap.
- very small p_T of the photoproduced system.

Dilepton production in semi-central collisions

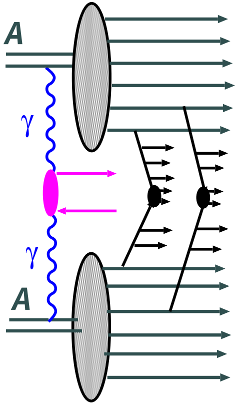

- dileptons from $\gamma\gamma$ fusion have peak at very low pair transverse momentum.
- can they be visible even in semi-central collisions?
- WW photons are a coherent “parton cloud” of nuclei, which can collide and produce particles. Nuclei create an “underlying event, in which e.g. plasma can be formed.
- Early considerations in N. Baron and G. Baur, Z. Phys. C **60** (1993).
- a first hint of the relevance of photoproduction mechanisms: a strong enhancement of J/ψ with $P_T < 300\,\mathrm{MeV}$ in peripheral reactions: J. Adam *et al.* [ALICE], Phys. Rev. Lett. **116** (2016) (for early estimates, see M. Kłusek-Gawenda and A. Szczurek, Phys. Rev. C **93** (2016)).
- Dileptons are a “classic” probe of the QGP: medium modifications of ρ, thermal dileptons... What is the competition between the different mechanisms?

Dilepton production in semi-central collisions

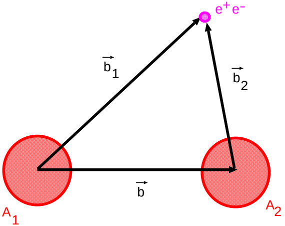

$$\frac{d\sigma_{ll}}{d\xi d^2\boldsymbol{b}} = \int d^2\boldsymbol{b}_1 d^2\boldsymbol{b}_2\, \delta^{(2)}(\boldsymbol{b} - \boldsymbol{b}_1 - \boldsymbol{b}_2) N(\omega_1, b_1) N(\omega_2, b_2) \frac{d\sigma(\gamma\gamma \to l^+l^-; \hat{s})}{d(-\hat{t})} \;,$$

where the phase space element is $d\xi = dy_+ dy_- dp_t^2$ with $y_\pm$, p_t and m_l the single-lepton rapidities, transverse momentum and mass, respectively, and

$$\omega_1 = \frac{\sqrt{p_t^2 + m_l^2}}{2}\left(e^{y_+} + e^{y_-}\right) \;,\; \omega_2 = \frac{\sqrt{p_t^2 + m_l^2}}{2}\left(e^{-y_+} + e^{-y_-}\right) \;,\; \hat{s} = 4\omega_1\omega_2 \;.$$

- we adopt the impact parameter definition of centrality

$$\frac{dN_{ll}[\mathcal{C}]}{dM} = \frac{1}{f_{\mathcal{C}} \cdot \sigma_{\rm AA}^{\rm in}} \int_{b_{\rm min}}^{b_{\rm max}} db \int d\xi\, \delta(M - 2\sqrt{\omega_1\omega_2})\, \frac{d\sigma_{ll}}{d\xi db}\Big|_{\rm cuts} \;,$$

Centrality

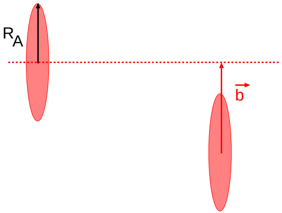

- e.g. from optical limit of Glauber:

$$\frac{d\sigma_{\mathrm{AA}}^{\mathrm{in}}}{db} = 2\pi b(1 - e^{-\sigma_{\mathrm{NN}}^{\mathrm{in}} T_{\mathrm{AA}}(b)})$$

  $\sigma_{\mathrm{AA}}^{\mathrm{in}} \sim 7\,\mathrm{barn}$ for Pb at LHC.
- fraction of inelastic hadronic events contained in the centrality class $\mathcal{C}$,

$$f_{\mathcal{C}} = \frac{1}{\sigma_{\mathrm{AA}}^{\mathrm{in}}} \int_{b_{\mathrm{min}}}^{b_{\mathrm{max}}} db \frac{d\sigma_{\mathrm{AA}}^{\mathrm{in}}}{db} \,.$$

- experimentally, centrality is determined by binning in multiplicity and/or transverse energy.

Dilepton production: impact parameter distribution

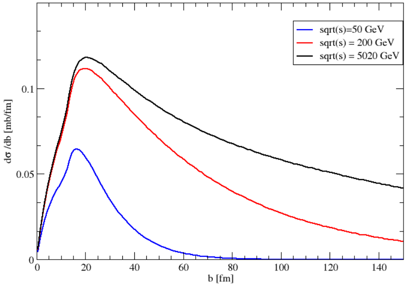

- semi-central collisions are situated on the left side of the distribution, below $b < 15\mathrm{fm}$.
- starting from RHIC energies, the contribution from coherent photons is practically energy-independent.
- also notice the long tails of the ultraperipheral part. Their importance rises with energy.

Thermal dilepton production

- The calculation of thermal dilepton production from a near-equilibrated medium follows the approach of R. Rapp and E. V. Shuryak, Phys. Lett. B **473** (2000); J. Ruppert, C. Gale, T. Renk, P. Lichard and J. I. Kapusta, Phys. Rev. Lett. **100** (2008). R. Rapp and H. van Hees, Phys. Lett. B **753** (2016) 586.
- To compute dilepton invariant-mass spectra an integration of the thermal emission rate over the space-time evolution of the expanding fireball is performed,

$$\frac{dN_{ll}}{dM} = \int d^4x \, \frac{M d^3P}{P_0} \, \frac{dN_{ll}}{d^4x d^4P} \; ,$$

  where $(P_0, \vec{P})$ and $M = \sqrt{P_0^2 - P^2}$ are the 4-vector $(P = |\vec{P}|)$ and invariant mass of the lepton pair, respectively.
- The thermal emission rate is expressed through the EM spectral function,

$$\frac{dN_{ll}}{d^4x d^4P} = \frac{\alpha_{\mathrm{EM}}^2 L(M)}{\pi^3 M^2} \, f^B(P_0; T) \, (-g_{\mu\nu}) \mathrm{Im}\Pi_{\mathrm{EM}}^{\mu\nu}(M, P; \mu_B, T) \; ,$$

- The fireball evolves through both QGP and hadronic phases. For the respective spectral functions we employ in-medium quark-antiquark annihilation and in-medium vector spectral functions in the hadronic sector.
- Different centrality classes for different colliding systems are characterized by the measured hadron multiplicities and appropriate initial conditions for the fireball.

Dilepton production in semi-central collisions

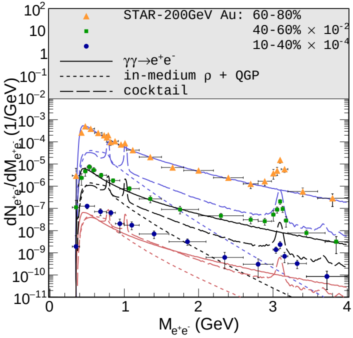

Left panel: Dielectron invariant-mass spectra for pair-$P_T<0.15$ GeV in Au+Au($\sqrt{s_{NN}}$=200 GeV) collisions for 3 centrality classes including experimental acceptance cuts ($p_t>0.2$ GeV, $|\eta_e|<1$ and $|y_{e^+e^-}|<1$) for $\gamma\gamma$ fusion (solid lines), thermal radiation (dotted lines) and the hadronic cocktail (dashed lines); right panel: comparison of the total sum (solid lines) to STAR data [1].

[1] data from J. Adam *et al.* [STAR Collaboration], Phys. Rev. Lett. **121** (2018) 132301.

- also added is a contribution from decays of final state hadrons "cocktail" supplied by STAR.
- the J/ψ contribution has been described e.g. in W. Zha, L. Ruan, Z. Tang, Z. Xu and S. Yang, Phys. Lett. B **789** (2019), 238-242 [arXiv:1810.02064 [hep-ph]].

Pair transverse momentum distribution

- Here we perform a simplified calculation by using b-integrated transverse momentum dependent photon fluxes,

$$\frac{dN(\omega, q_t^2)}{d^2\vec{q}_t} = \frac{Z^2\alpha_{EM}}{\pi^2}\frac{q_t^2}{[q_t^2+\frac{\omega^2}{\gamma^2}]^2}F^2_{\rm em}(q_t^2+\frac{\omega^2}{\gamma^2}).$$

$$\frac{d\sigma_{ll}}{d^2\vec{P}_T} = \int \frac{d\omega_1}{\omega_1}\frac{d\omega_2}{\omega_2} d^2\vec{q}_{1t} d^2\vec{q}_{2t} \frac{dN(\omega_1, q_{1t}^2)}{d^2\vec{q}_{1t}}\frac{dN(\omega_2, q_{2t}^2)}{d^2\vec{q}_{2t}}\delta^{(2)}(\vec{q}_{1t}+\vec{q}_{2t}-\vec{P}_T)\hat{\sigma}(\gamma\gamma\to l^+l^-)\Big|_{\rm cuts}$$

- analogous to TMD-factorization in hard processes. Note that experiment includes a cut $p_t(\mathrm{lepton}) > 0.2\,\mathrm{GeV}$. Formfactors ensure that photon virtualities are much smaller then this "hard scale". We can thus treat them as on-shell in the $\gamma\gamma \to e^+e^-$ cross section.
- notice the extremely sharp peak in q_t, which is cut off only by ω/γ. The peak will move towards smaller q_t as the boost γ increases.

Dilepton production in semi-central collisions

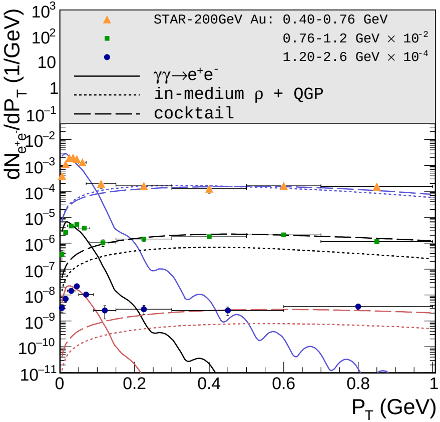

P_T spectra of the individual contributions (line styles as in the previous figure) in 3 different mass bins for 60-80% central Au+Au collisions ($\sqrt{s_{NN}}$=200 GeV), compared to STAR data [1].

[1] J. Adam *et al.* [STAR Collaboration], Phys. Rev. Lett. **121** (2018) 132301.

Dilepton production in semi-central collisions

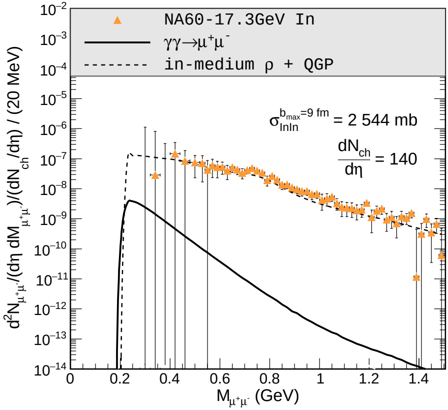

Low-P_T ($<$0.2 GeV) acceptance-corrected dimuon invariant mass excess spectra in the rapidity range $3.3 < Y_{\mu^+\mu^-,LAB} < 4.2$ for MB In+In ($\sqrt{s_{NN}}$=17.3 GeV) collisions at the SPS. Calculations for coherent $\gamma\gamma$ fusion (solid line) and thermal radiation (dashed line) are compared to NA60 data [1].

[1] R. Arnaldi *et al.* [NA60 Collaboration], Eur. Phys. J. C **61** (2009) 711.

Dilepton production in semi-central collisions

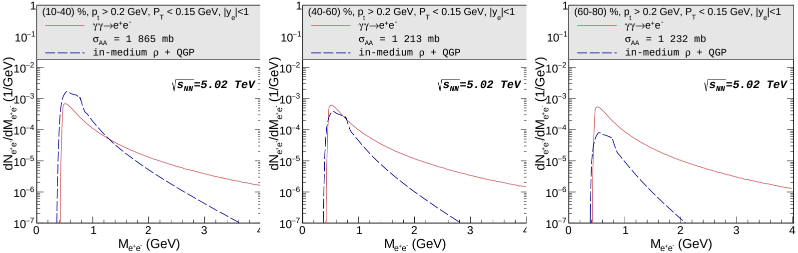

Our predictions for low-P_T dilepton radiation in Pb+Pb ($\sqrt{s_{NN}}$=5.02 TeV) collisions from coherent $\gamma\gamma$ fusion (solid lines) and thermal radiation (dashed lines) for three centrality classes and acceptance cuts as specified in the figures.

Dilepton production in semi-central collisions

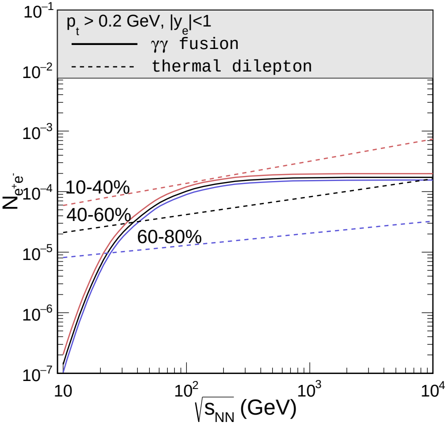

Excitation function of low-P_T ($<0.15\,$GeV) dilepton yields from $\gamma\gamma$ fusion (solid lines) and thermal radiation (dashed lines) in collisions of heavy nuclei (A$\simeq$200) around midrapidity in three centrality classes, including single-$e^{\pm}$ acceptance cuts.

Density matrix approach, (M. Kłusek-Gawenda, WS, A. Szczurek, in preparation)

- Electric field vector

$$\boldsymbol{E}(\omega, \boldsymbol{q}) \propto \frac{\boldsymbol{q} F(q^2)}{\boldsymbol{q}^2 + \frac{\omega^2}{\gamma^2}}$$

- Then we introduce the Wigner-type density matrix

$$N_{ij}(\omega, \boldsymbol{b}, \boldsymbol{q}) = \int \frac{d^2\boldsymbol{Q}}{(2\pi)^2} \exp[-i\boldsymbol{b}\boldsymbol{Q}]\, E_i\left(\omega, \boldsymbol{q} + \frac{\boldsymbol{Q}}{2}\right) E_j^*\left(\omega, \boldsymbol{q} - \frac{\boldsymbol{Q}}{2}\right)$$

  when summed over polarizations it reduces to the well-known WW flux after integrating over $\boldsymbol{q}$, and to the TMD photon flux after integrating over $\boldsymbol{b}$.
- cross section:

$$\begin{aligned} d\sigma &= \int d^2\boldsymbol{b}_1 d^2\boldsymbol{b}_2\, \delta^{(2)}(\boldsymbol{b} - \boldsymbol{b}_1 + \boldsymbol{b}_2) \int \frac{d\omega_1}{\omega_1} \frac{d\omega_2}{\omega_2} d^2\boldsymbol{q}_1 d^2\boldsymbol{q}_2\, \delta^{(2)}(\boldsymbol{P} - \boldsymbol{q}_1 - \boldsymbol{q}_2) \\ &\times N_{ij}(\omega_1, \boldsymbol{b}_1, \boldsymbol{q}_1) N_{kl}(\omega_2, \boldsymbol{b}_2, \boldsymbol{q}_2)\, \frac{1}{2\hat{s}} M_{ik} M_{jl}^\dagger\, d\Phi(l^+ l^-). \end{aligned}$$

- no independent sum over photon polarizations!
- other approaches: M. Vidovic, M. Greiner, C. Best and G. Soff, Phys. Rev. **C47** (1993); K. Hencken, G. Baur and D. Trautmann, Phys. Rev. C **69** (2004) 054902; S. Klein et al. (2020).

Density matrix approach

$$\begin{aligned}\frac{d\sigma}{d^2\boldsymbol{b}d^2\boldsymbol{P}} &= \int \frac{d^2\boldsymbol{Q}}{(2\pi)^2}\exp[-i\boldsymbol{b}\boldsymbol{Q}]\int \frac{d\omega_1}{\omega_1}\frac{d\omega_2}{\omega_2}\int \frac{d^2\boldsymbol{q}_1}{\pi}\frac{d^2\boldsymbol{q}_2}{\pi}\,\delta^{(2)}(\boldsymbol{P}-\boldsymbol{q}_1-\boldsymbol{q}_2)\\ &\times \; E_i\left(\omega_1,\boldsymbol{q}_1+\frac{\boldsymbol{Q}}{2}\right)E_j^*\left(\omega_1,\boldsymbol{q}_1-\frac{\boldsymbol{Q}}{2}\right)E_k\left(\omega_2,\boldsymbol{q}_2-\frac{\boldsymbol{Q}}{2}\right)E_l^*\left(\omega_2,\boldsymbol{q}_2+\frac{\boldsymbol{Q}}{2}\right)\\ &\times \; \frac{1}{2\hat{s}}\sum_{\lambda\bar{\lambda}} M_{ik}^{\lambda\bar{\lambda}}M_{jl}^{\lambda\bar{\lambda}\dagger}\,d\Phi(l^+l^-).\end{aligned}$$

with

$$\begin{aligned}\sum_{\lambda\bar{\lambda}} M_{ik}^{\lambda\bar{\lambda}}M_{jl}^{\lambda\bar{\lambda}\dagger} &= \delta_{ik}\delta_{jl}\sum_{\lambda\bar{\lambda}}\left|M_{\lambda\bar{\lambda}}^{(0,+)}\right|^2+\epsilon_{ik}\epsilon_{jl}\sum_{\lambda\bar{\lambda}}\left|M_{\lambda\bar{\lambda}}^{(0,-)}\right|^2\\ &+ \; P_{ik}^{\parallel}P_{jl}^{\parallel}\sum_{\lambda\bar{\lambda}}\left|M_{\lambda\bar{\lambda}}^{(2,-)}\right|^2+P_{ik}^{\perp}P_{jl}^{\perp}\sum_{\lambda\bar{\lambda}}\left|M_{\lambda\bar{\lambda}}^{(2,+)}\right|^2\end{aligned}$$

$$\delta_{ik} = \hat{x}_i\hat{x}_k+\hat{y}_i\hat{y}_k,\;\; \epsilon_{ik}=\hat{x}_i\hat{y}_k-\hat{y}_i\hat{x}_k,\;\; P_{ik}^{\parallel}=\hat{x}_i\hat{x}_k-\hat{y}_i\hat{y}_k,\;\; P_{ik}^{\perp}=\hat{x}_i\hat{y}_k+\hat{y}_i\hat{x}_k$$

- In the $\gamma\gamma$ CM, colliding photons can be in the $J_z = 0, \pm 2$ states.

Dilepton production in semi-central collisions (preliminary)

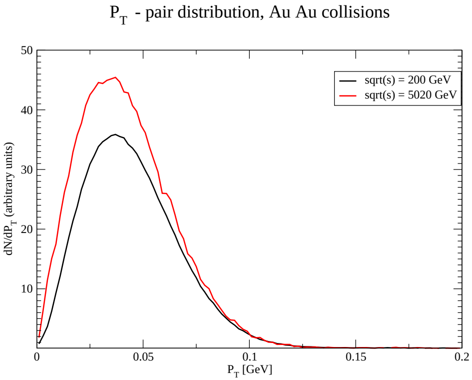

P_T spectra for 60-80% central Au+Au collisions ($\sqrt{s_{NN}}$=200 GeV, 5020 GeV).

- peak does not run away to $P_T \to 0$ with increasing energy, as in the naive TMD approach.

Summary

- We have studied low-P_T dilepton production in ultrarelativistic heavy-ion collisions, by a systematic comparisons of thermal radiation and photon-photon fusion within the coherent fields of the incoming nuclei.
- Comparison to recent STAR data: good description of low-P_T dilepton data in Au-Au($\sqrt{s_{NN}}$=200 GeV) collisions in three centrality classes, for invariant masses from threshold to $\sim$4 GeV.
- Coherent emission dominant for the two peripheral samples, and comparable to the cocktail and thermal radiation yields in semi-central collisions.
- At SPS energies ($\sqrt{s_{NN}}$=17.3 GeV) we found that the $\gamma\gamma$ contribution is subleading. Only relevant at low P_T and near the dimuon threshold, rapidly falling off with increasing mass.
- Impact-parameter dependent dilepton P_T distribution is described by a density matrix generalization of the Weizsäcker-Williams fluxes. Different weights of $J_z = 0, \pm 2$ channels of the $\gamma\gamma$-system. For e^+e^- pairs the $J_z = \pm 2$ channels dominate.